Journal of Materials Chemistry A

Suppressing Hydrogen Evolution at Catalytic Surfaces in the Aqueous Lithium Ion Batteries

Journal:	*Journal of Materials Chemistry A*
Manuscript ID	TA-COM-06-2020-005568.R1
Article Type:	Communication
Date Submitted by the Author:	03-Jul-2020
Complete List of Authors:	Wang, Fei; Fudan University, Department of Materials Science Lin, Chuan-Fu ; The Cathode University of America; University of Maryland, Department of Materials Science and Engineering Ji, Xiao; University of Maryland, Department of Chemical & Biomolecular Engineering Rubloff, Gary; University of Maryland, Materials Science and Engineering; University of Maryland Wang, Chunsheng; University of Maryland, Department of Chemical & Biomolecular Engineering

Suppressing Hydrogen Evolution at Catalytic Surfaces in the Aqueous Lithium Ion Batteries

Fei Wang,[1+] *Chuan-Fu Lin,*[2,3+] *Xiao Ji,*[4+] *Gary W. Rubloff,*[2] *and Chunsheng Wang**[4,5]

1. Department of Materials Science, Fudan University, Shanghai, 200433, China
2. Department of Materials Science and Engineering, University of Maryland, College Park, MD 20742, USA
3. Department of Mechanical Engineering, The Cathode University of America, Washington, DC 20064, USA
4. Department of Chemical and Biomolecular Engineering, University of Maryland, College Park, MD 20742, USA
5. Department of Chemistry and Biochemistry, University of Maryland, College Park, MD 20742, USA

Corresponding Author
Fei Wang, E-mail: feiw@fudan.edu.cn
Chunsheng Wang, E-mail: cswang@umd.edu

ABSTRACT

Aqueous lithium ion batteries (ALIBs) have attracted increasing attentions due to their high safety. The water-in-salt electrolyte (WISE) enabled a wider voltage window (3.0 V) through the formation of solid-electrolyte-interphase (SEI) on the anode. However, the cathodic limit of WiSE and its derivatives still cannot effectively support the desired energy dense anodes, such as $Li_4Ti_5O_{12}$ (LTO). At the anode, the hydrogen evolution reaction (HER) is the main parasitic process that competes with the desired lithiation process therein. In this work, we investigated the catalytic activity of different coating layers and put forward the selection criterion for the surface layers. We demonstrated that Al_2O_3 is such a surface that effectively suppresses HER and enables the cycling of LTO anode in WiSE, delivering a capacity of 145 mAh/g. Such understanding provides important guidelines for designing future electrolytes and interphases for aqueous battery chemistries.

Aqueous lithium ion batteries (ALIBs) are promising energy storage technology due to their non-flammable nature, the capability to be manufactured in the ambient environment, and the low reliance on the battery management systems at the module or pack levels[1-5]. However, traditional ALIBs are limited by their inferior energy densities, which is primarily caused by the narrow electrochemical stability window of water (1.23 V)[3, 6]. Recently, the expanded stability window (3.0 V) of the so-called "water-in-salt" electrolyte (WiSE) overcame this restriction and enabled a series of high voltage/energy aqueous battery chemistries that were once prohibited in the aqueous systems [4, 7-10]. The expansion of the cathodic limit by 0.6 V was realized by the formation of a solid-electrolyte-interphase (SEI) on the anode surface derived from the reduction of salt anions and overall reduction of water activity[9, 11]. However, since the cathodically-polarized anode surface would repel the anions away from the inner-Helmholtz layer of the surface, further expansion of the cathodic limits via anion-reduction becomes very challenging even with a higher concentration[11, 12]. As a result, the cathodic limit of the WiSE is still not low enough to support the anode materials such as $Li_4Ti_5O_{12}$ (LTO), whose redox potential is 1.55 V vs Li and sits near the cathodic limit of WiSE[13].

The passivation capability of SEI formed in most non-aqueous electrolytes enables a cathodic stability limit well below 1.0V, which is obviously more effective than anion-derived SEIs formed in WiSE [14-18]. Apparently, the chemical nature of the SEI is critical for expansion of electrolyte stability window. The primary criterion for an effective SEI is its electrolyte nature, i.e., insulating electrons while conducting ions of significance to the cell reactions [17, 19-22]; for aqueous systems, this criterion can be translated into low catalytic activity for the hydrogen evolution reaction (HER), since the HER is the main parasitic process at anode and competes with the desired lithiation process therein. While suppressing the HER catalytic activity of the zinc metal anode in the aqueous batteries is regarded as effective to avoid water decomposition[23-26], kinetically suppressing HER of LTO anode is rarely investigated by the scientists from battery perspective. On the other hand, HER have been intensely investigated, with a purpose quite the opposite, i.e., splitting water electrochemically, whose behavior is represented by the well-known volcano plot [27-35]. Thus, reversed use of the traditional volcano plot could help us find that materials that is least catalytic for HER, which in theory could serve as an electrode surface friendly to SEI growth.

In this work, guided by the theoretical calculation using the Gibbs free energy for atomic hydrogen adsorption (ΔG_H) and density of states (DOS), we investigate the electrochemical performances of uncoated, Al_2O_3, ZnO and TiO_2-coated LTO electrodes in the WISE. We demonstrated that Al_2O_3 is such a surface that effectively suppresses HER and enables the cycle of LTO anode in WiSE, delivering a capacity of 145 mAh/g. This selection criterion for SEI-friendly surface in aqueous electrolyte provides a novel approach to engineer interphases for next generation battery chemistries.

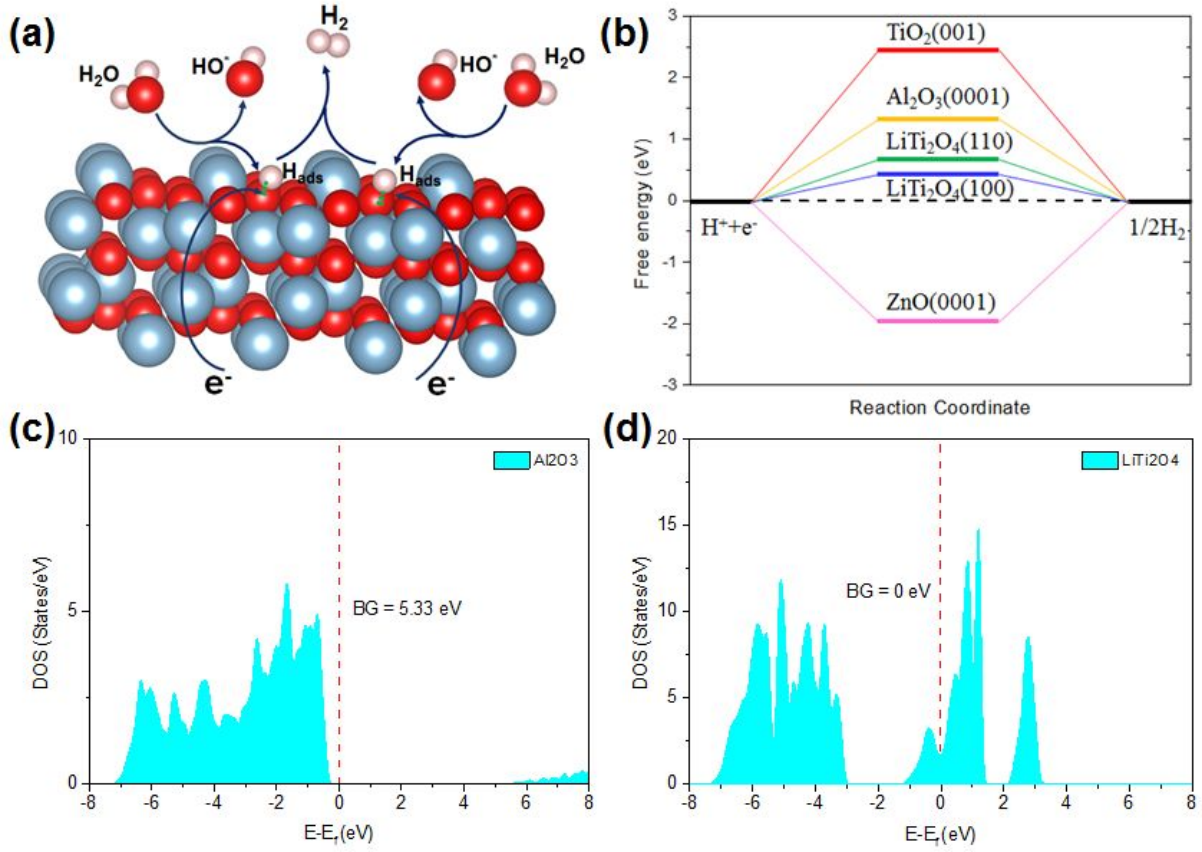

Figure 1. (a) The schematic illustration of the HER process on the electrode/electrolyte interfaces. (b) The simulation results of the free energy of adsorption of hydrogen (ΔG_H) for the different surface coatings. The density of state for (c) Al_2O_3 and (d) $LiTi_2O_4$. The red dash lines indicate the Fermi energies, and the band gaps (BG) are listed.

When evaluated as the electrode substrate in WiSE, various metallic current collectors demonstrate completely different cathodic stability limits, which, as determined by the HER potentials, increases by the order of Al<Ti<SS<Carbon<Cu<Ni (Figure S1), and are well

consistent with the volcano curve reported for the HER on metal electrodes. This suggests that there should be a correlation between metal surface passivation and the reduction in their catalytic activities [28, 34]. In particular, the reduction onset potential for Al is significantly lower than the others, indicating a possible combined contribution of its inherent low catalytic activity and the dense surface passivation. Although as a common practice the electrochemical stability window of electrolytes is typically assessed using linear sweep technique on non-porous electrode surfaces, such window varies significantly with the electrode materials. The difference could be pronounced, especially if the electrode materials used are composites such as those in real-life electrochemical devices [36], where appreciable amount of conductive carbon and polymer binder lead to much higher surface area and catalytic activities than non-porous metal surfaces. As a result, the actual reduction or oxidation stabilities of an electrolyte in those devices will be largely affected by the surface properties of the carbon and active materials, with a minor contribution from the current collectors.

HER is a surface reaction that has been known to heavily depend on the interaction between the adsorbed hydrogen atom (H_{ads}) and the catalytic activity of the electrode surface (Figure 1a)[31, 35, 37]. Thus, to improve the performance of a battery anode in aqueous electrolytes, one must attempt the exact opposite of electrocatalysis, i.e., making the electrode surface as little catalytic as possible. Based on this line of thought, we sought to apply materials of "poor" catalytic activity as a conformal coating on electrode, which serves to physically prevent the direct contact between electrolyte and electrode.

Using DFT we calculated the free energy of hydrogen (ΔG_H) on various coating materials as well as their electronic conductivity, and use the two parameters to screen for the best candidate material. Since volcano plots state that the materials with suitable hydrogen adsorption (neither too strong nor too weak) locating at the top of the plots would have the optimum activity, then reversely, the materials with either very strong (highly negative $-\Delta G_H$) or very weak bonding (highly positive $+\Delta G_H$) should be ideal candidates to suppress HER. The high ΔG_H of Al_2O_3 (Figure 1b) suggests that its suitability, while TiO_2, despite its high ΔG_H, becomes highly catalytic toward HER once lithiated into $LiTi_2O_4$ that is characterized by a low ΔG_H. This increased catalytic activity with lithiation degree might explain why LTO in non-aqueous batteries effectively catalyzes the decomposition of trace H_2O existing in both electrodes and electrolyte. With highly

negative ΔG_H, ZnO would also serve as a good candidate for HER suppression, however, its high electronic conductivity accelerates the charge-transfer between electrolyte and electrodes, which kinetically favors the electrochemical reduction of water. On the contrary, Al_2O_3 has a rather large band-gap of 5.33 eV (Figure 1c), suggesting a very poor electrical conductivity that prevents the charge transfer, in sharp comparison with the band-gaps of lithiated $LiTi_2O_4$ (0 eV) and ZnO (1.48 eV), respectively. In fact, the latter two were well known for their metallic and semiconducting behaviors (Figure 1d and Figure S1). Therefore, the insulator Al_2O_3 makes the best candidate surface for HER suppression.

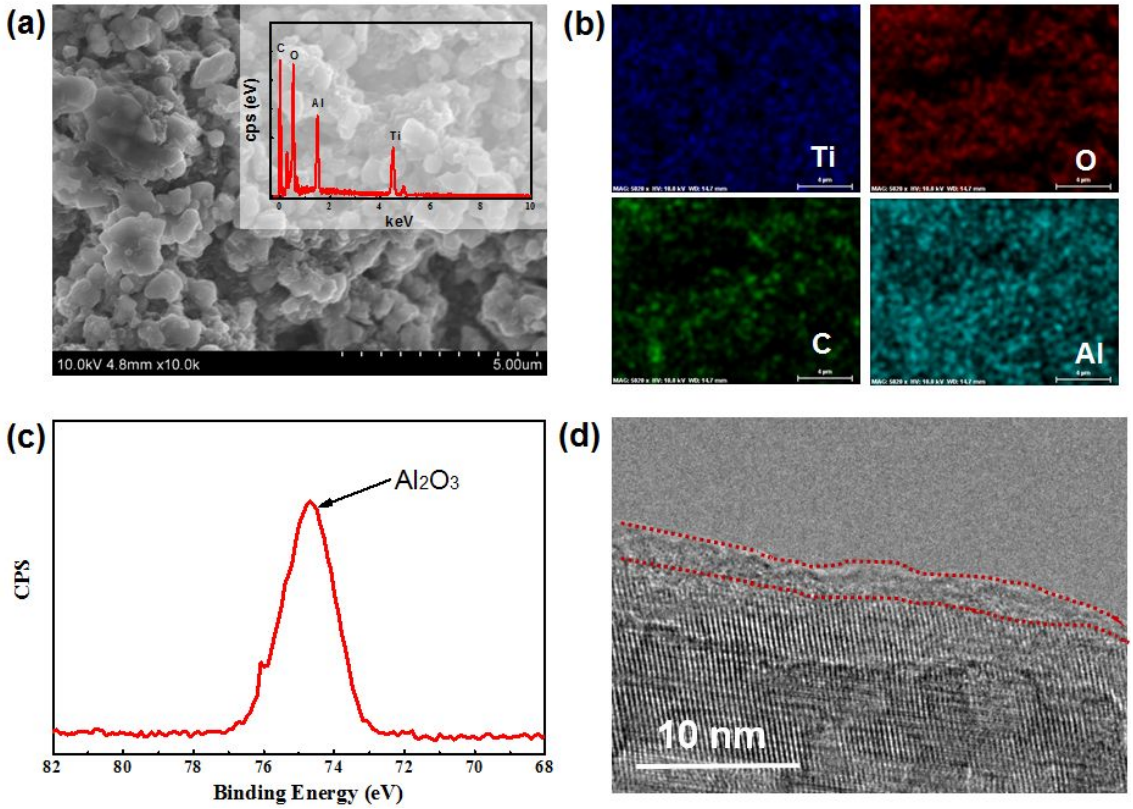

Figure 2. (a) The SEM image of the Al_2O_3 coated LTO electrode and the corresponding EDX results. (b) The element mapping, (c) the Al-XPS spectra and (d) the TEM image of the Al_2O_3 coated LTO electrode.

An Al_2O_3 layer with a nanometric thickness was coated on an LTO electrode using atomic layer deposition (ALD) technique. As shown in the scanning electron microscope (SEM) image (Figure 2a), LTO maintains the particle morphology and crystallinity after coating. Energy Dispersive X-Ray Analysis (EDX) confirms the existence of Al on the electrode surface. The uniform distribution of Al in elements mappings (Figure 2b) reveals that the electrode surface was

uniformly covered by Al_2O_3. The Al_{2p} peak at ~74.8 eV in X-ray photoelectron spectroscopy (XPS, Figure 2c) is well indexed to Al_2O_3. The thickness of the coating was determined to be ~3 nm by transmission electron microscopy (TEM) (Figure 2d). An additional peak at ~350 cm^{-1} [38] in Raman spectroscopy (Figure S2) in comparison with pristine LTO also confirms the existence of Al_2O_3 coating.

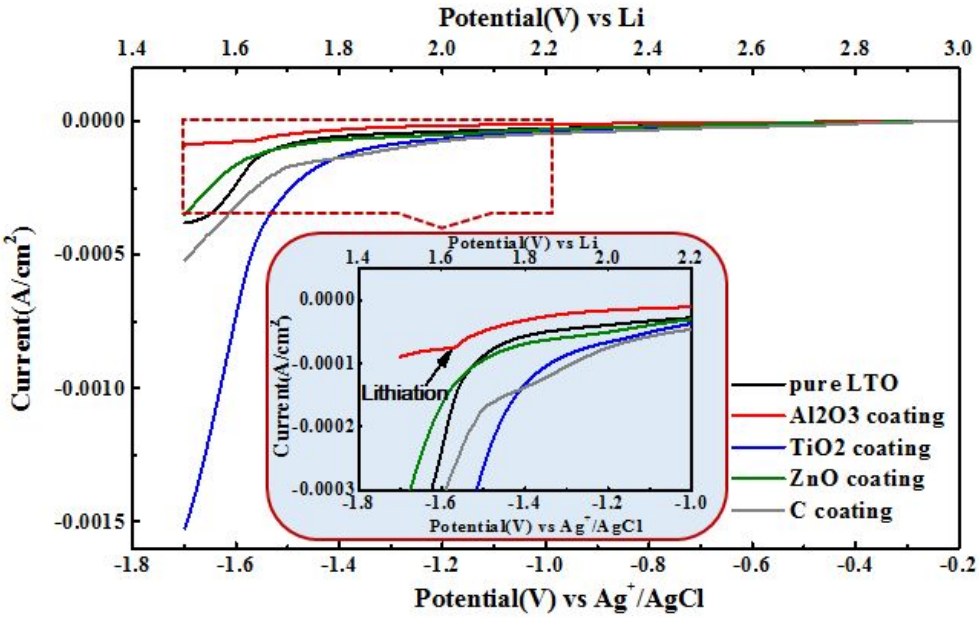

Figure 3. The cathodic limits evaluated by linear sweep voltammetry on LTO surfaces coated with different materials (inset the enlarged view). Counter electrode: activated carbon; Reference electrode: Ag/AgCl; Scan rate: 1 mV/s.

The electrochemical performance of LTO electrodes coated with various materials was evaluated by linear sweep (Figure 3). The hydrogen evolution begins at ~1.8 V vs Li on pristine LTO surface, which is higher than its lithiation potential (1.55V). The HER process rather than lithiation of LTO dominates the cathodic reaction during the scan. The carbon-coating enhances the electronic conductivity of LTO, thus accelerating the HER reactions as evidenced by the higher currents and positively shifted HER potential. TiO_2-coating also positively shifts the cathodic limit due to its high catalytic activity. By contrast, both ZnO- and Al_2O_3-cotings negatively shift the cathodic limit potential by 0.1V. In addition, the HER currents on ZnO- and Al_2O_3-coated LTO electrode are also much lower compared with the pristine LTO. The HER suppression capability as quantified by the onset potential of HER should increase in the order of TiO_2<C<LTO<ZnO<Al_2O_3, which is consistent with what predicted in Figure 1. The Al_2O_3-

coating not only suppresses the HER catalytic activity but also acts as a kinetic barrier to slow down the electron transfer from electrode bulk to the proton in the electrolyte[39]. Since Al_2O_3-coating successfully shifts the HER potential to <1.5 V, thus Li^+-intercalation is enabled before HER, as evidenced by a sharp lithiation peak at 1.55 V (Figure 4a). In similar approaches, we also evaluated the effect of surface coating on oxygen evolution reaction (OER). Al_2O_3- and TiO_2-coating on $LiNi_{0.5}Mn_{1.5}O_4$ only slightly reduces the side reactions on this high voltage (4.8 V) cathode material (Figure S3).

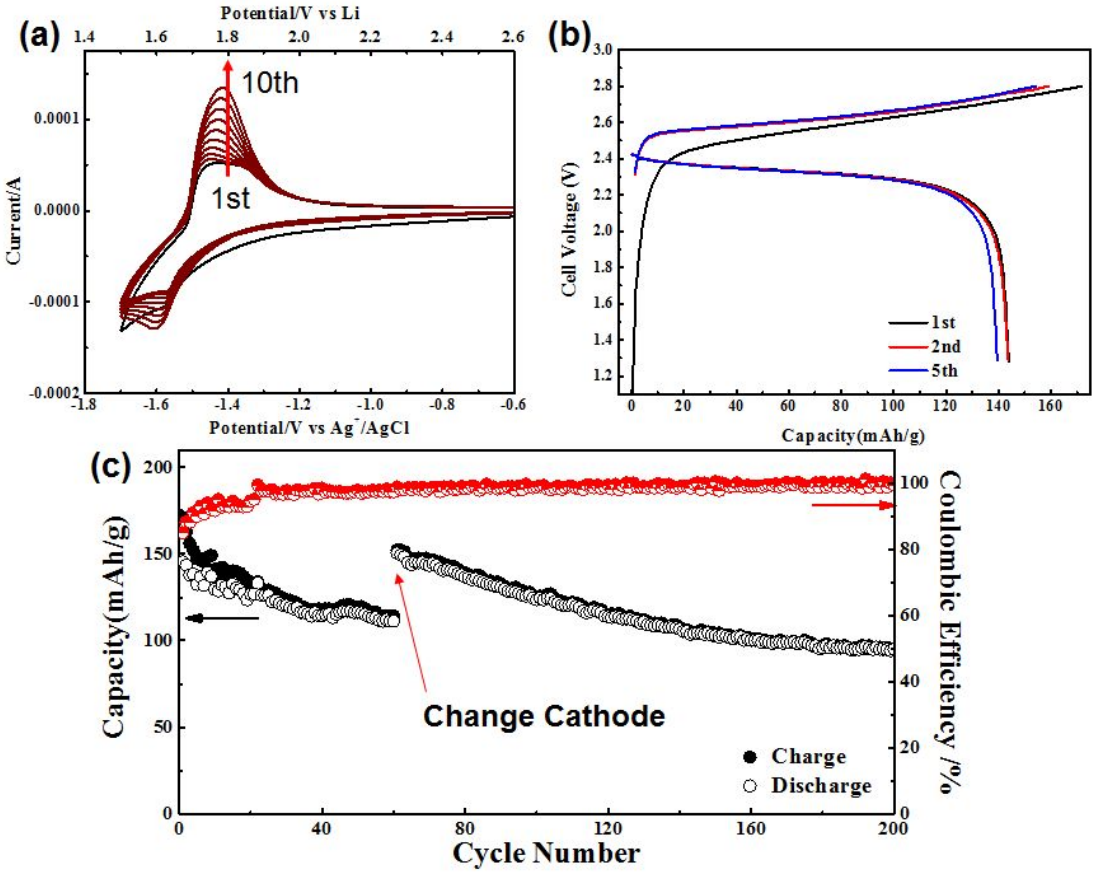

Figure 4. a) Cyclic voltammetry (CV) scan of Al_2O_3-coated LTO anodes in water-in-salt in electrolytes at the scanning rate of 5 mV/S using an activated carbon counter electrode and an Ag/AgCl reference. b) The voltage profile of the full cell using Al_2O_3-coated LTO anode and LMO cathode at 1 C current. c) The cycling performance of the full cell using Al_2O_3-coated LTO anode and LMO cathode.

As shown in the CV curves of Al_2O_3-coated (Figure 4a) and pristine LTO (Figure S4), the oxidative current peak at 1.8 V is clearly observed on the former, and it increases with the cycling, while very low oxidation current is detected on pristine LTO. Therefore Al_2O_3-coating on LTO

effectively suppressed the HER and Li^+-diffusion in Al_2O_3 is gradually activated during the initial few CV scans [39-41].

$LiMn_2O_4$ (LMO) was used as a cathode to evaluate the electrochemical performance of Al_2O_3-coated LTO in the WiSE (Figure S5). The LMO/LTO mass ratio was set as 2.5:1 to accommodate the low CE of LTO during the initial several cycles. 1 C was used instead of the high rate to demonstrate the stability of electrolyte in the full cell. Such LTO/LMO full cell delivers a voltage plateau at ~2.4 V during the discharging process. The discharging capacity based on LTO mass is 145 mAh/g. In the first cycle, a coulombic efficiency of 84.5% was delivered, indicating a relatively low amount of electrolyte was consumed to form additional LiF-rich SEI on the Al_2O_3-coated LTO anode. In comparison, pairing the uncoated LTO and LMO only delivered a low CE of 50% (Figure S6), further confirming the effect of the Al_2O_3 coating in suppressing the side reaction. As reported in our previous work, the reductions of salt anions bis(trifluoromethane sulfonyl)imide (TFSI) happens between 1.9 ~ 2.9 V[4]. Although the reduction of TFSI anions are still expected to happen when there is no Al_2O_3 coating (Figure S7), the formation of complete SEI needs long time (i.e few cycles in galvanostatic charge/discharge cycles). Since lithiation potential of pristine LTO resides beyond the cathodic limit of WiSE, significant HER will happen before the lithiation. The persistent gas evolution undoubtedly prevents complete SEI formation. For the initial cycles where the robust SEI has not been constructed, the protection of Al_2O_3 surface serves as a key barrier to ensure that SEI chemistry occurs, and the SEI ingredient formed from the reduction of TFSI anion adhere to anode surface. After the most challenging period in the initial cycles, dense and complete SEI will come into shape (Figure S7), eventually providing long-term protection and allowing LTO to deliver a reversible capacity.

The cycling performance of LTO/LMO full cell is shown in Figure 4c. The capacity of LTO/LMO full cell gradually decrease rapidly, while the Coublmbic efficiency (CE) increased from 84.5% to ~99% after 60 cycles. The decay should be induced by the persistent consumption of Li source from LMO, as indicated by the low CE[42]. After taking apart the cycled cell and replenishing a fresh LMO cathode, the cell capacity recovered to 150 mAh/g from 106 mAh/g, confirming that the capacity decay was indeed due to the excessive Li consumption, while LTO itself is chemically stable in the aqueous electrolytes. The cycle performance could thus be

extended to 200 cycles. More efficient surface passivation using new coating materials holds the potential to further optimize the LTO electrode for superior performance.

In summary, we investigated how to suppress the surface HER activity to enable the reversible lithiation/de-lithiation reactions of LTO anode in aqueous electrolytes. Combining the simulation and the experiment results, Al_2O_3 was identified to be an optimum surface passivation material, based on its high ΔG_H and low electronic conductivity. Dramatic electrochemical performance improvement has been realized with Al_2O_3-coating on the LTO electrode via ALD. The Li-ion full cell constructed with LTO and LMO delivered a high working voltage of 2.4 V for 200 cycles. More importantly, we raised the importance of catalytic electrode surface in dictating the electrochemical stability of electrolyte materials. The work could also impact other aqueous or non-aqueous devices that face similar challenges.

Author Contribution

F.Wang, C.Lin and X. Ji contributed equally to this work

Acknowlegements

We acknowledge the support of the Maryland Nano Center and its NispLab. The NispLab is supported in part by the NSF as a MRSEC Shared Experimental Facility. C.-F.L. and G.W.R are supported by Nanostructures for Electrical Energy Storage (NEES) funded by U.S Department of Energy, Office of Science, Office of Basic Energy Sciences under Award Number DESC0001160.

Reference

1. F. Wang, L. Suo, Y. Liang, C. Yang, F. Han, T. Gao, W. Sun and C. Wang, *Adv.Energy.Mater*, 2017, **7**.
2. F. Wang, Y. Lin, L. Suo, X. Fan, T. Gao, C. Yang, F. Han, Y. Qi, K. Xu and C. Wang, *Energy Environ. Sci.* , 2016, **9**, 3666-3673.
3. W. Li, J. R. Dahn and D. S. Wainwright, *Science*, 1994, **264**, 1115-1118.
4. L. Suo, O. Borodin, T. Gao, M. Olguin, J. Ho, X. Fan, C. Luo, C. Wang and K. Xu, *Science*, 2015, **350**, 938-943.
5. Y. Yamada, K. Usui, K. Sodeyama, S. Ko, Y. Tateyama and A. Yamada, *Nature Energy*, 2016, **1**, 16129.
6. J.-Y. Luo and Y.-Y. Xia, *Adv. Funct. Mater.* , 2007, **17**, 3877-3884.
7. L. Suo, O. Borodin, W. Sun, X. Fan, C. Yang, F. Wang, T. Gao, Z. Ma, M. Schroeder and A. von Cresce, *Angew. Chem. Int. Ed.* , 2016, **55**, 7136-7141.
8. L. Suo, O. Borodin, Y. Wang, X. Rong, W. Sun, X. Fan, S. Xu, M. A. Schroeder, A. V. Cresce and F. Wang, *Adv.Energy.Mater*, 2017, **7**.

9. L. Suo, D. Oh, y. lin, Z. Zhuo, O. Borodin, T. Gao, f. wang, A. Kushima, Z. Wang and H.-C. Kim, *J. Am. Chem. Soc.* , 2017.
10. F. Wang, O. Borodin, T. Gao, X. Fan, W. Sun, F. Han, A. Faraone, J. A. Dura, K. Xu and C. Wang, *Nat. Mater.* , 2018, 1.
11. F. Wang, O. Borodin, M. S. Ding, M. Gobet, J. Vatamanu, X. Fan, T. Gao, N. Edison, Y. Liang and W. Sun, *Joule*, 2018.
12. C. Yang, J. Chen, T. Qing, X. Fan, W. Sun, A. von Cresce, M. S. Ding, O. Borodin, J. Vatamanu and M. A. Schroeder, *Joule*, 2017, **1**, 122-132.
13. M. Börner, S. Klamor, B. Hoffmann, M. Schroeder, S. Nowak, A. Würsig, M. Winter and F. Schappacher, *J. Electrochem. Soc.*, 2016, **163**, A831-A837.
14. M. Steinhauer, S. Risse, N. Wagner and K. A. Friedrich, *Electrochim. Acta* 2017, **228**, 652-658.
15. Q. Zhang, J. Pan, P. Lu, Z. Liu, M. W. Verbrugge, B. W. Sheldon, Y.-T. Cheng, Y. Qi and X. Xiao, *Nano Lett.* , 2016, **16**, 2011-2016.
16. K. Xu, *Chem. Rev.* , 2014, **114**, 11503-11618.
17. K. Xu, *Chem. Rev.* , 2004, **104**, 4303-4417.
18. D. M. Seo, D. Chalasani, B. S. Parimalam, R. Kadam, M. Nie and B. L. Lucht, *ECS Electrochemistry Letters*, 2014, **3**, A91-A93.
19. X.-Y. Yue, X.-L. Li, W.-W. Wang, D. Chen, Q.-Q. Qiu, Q.-C. Wang, X.-J. Wu, Z.-W. Fu, Z. Shadike and X.-Q. Yang, *Nano Energy*, 2019, **60**, 257-266.
20. Y. Liu, D. Lin, P. Y. Yuen, K. Liu, J. Xie, R. H. Dauskardt and Y. Cui, *Adv. Mater.* , 2017, **29**.
21. N. W. Li, Y. X. Yin, C. P. Yang and Y. G. Guo, *Adv. Mater.* , 2016, **28**, 1853-1858.
22. M. Gauthier, T. J. Carney, A. Grimaud, L. Giordano, N. Pour, H. H. Chang, D. P. Fenning, S. F. Lux, O. Paschos, C. Bauer, F. Maglia, S. Lupart, P. Lamp and Y. Shao-Horn, *J. Phys. Chem. Lett.* , 2015, **6**, 4653-4672.
23. K. Wongrujipairoj, L. Poolnapol, A. Arpornwichanop, S. Suren and S. Kheawhom, *physica status solidi (b)*, 2017, **254**, 1600442.
24. H. He, H. Tong, X. Song, X. Song and J. Liu, *J. Mater. Chem. A*, 2020, **8**, 7836-7846.
25. Y.-D. Cho and G. T.-K. Fey, *J. Power Sources* 2008, **184**, 610-616.
26. Y. Zhang, Y. Wu, W. You, M. Tian, P. W. Huang, Y. Zhang, Z. Sun, Y. Ma, T. Hao and N. Liu, *Nano Lett.* , 2020, **20**, 4700-4707.
27. P. Quaino, F. Juarez, E. Santos and W. Schmickler, *Beilstein journal of nanotechnology*, 2014, **5**, 846-854.
28. Y. Fujimori, W. E. Kaden, M. A. Brown, B. Roldan Cuenya, M. Sterrer and H.-J. Freund, *The Journal of Physical Chemistry C*, 2014, **118**, 17717-17723.
29. T. F. Jaramillo, K. P. Jørgensen, J. Bonde, J. H. Nielsen, S. Horch and I. Chorkendorff, *science*, 2007, **317**, 100-102.
30. J. Greeley, T. F. Jaramillo, J. Bonde, I. B. Chorkendorff and J. K. Norskov, *Nat. Mater.* , 2006, **5**, 909-913.
31. B. Conway and B. Tilak, *Electrochim. Acta* 2002, **47**, 3571-3594.
32. B. Conway and G. Jerkiewicz, *Solid State Ionics* 2002, **150**, 93-103.
33. L. Scatena, M. Brown and G. Richmond, *Science*, 2001, **292**, 908-912.
34. M. Jaksic, *J. New Mater. Electrochem. Syst.* , 2000, **3**, 153-168.
35. J. Barber, S. Morin and B. Conway, *J. Electroanal. Chem.* , 1998, **446**, 125-138.
36. F. Han, Y. Zhu, X. He, Y. Mo and C. Wang, *Adv.Energy.Mater*, 2016, **6**, 1501590.
37. D. Strmcnik, P. P. Lopes, B. Genorio, V. R. Stamenkovic and N. M. Markovic, *Nano Energy*, 2016, **29**, 29-36.
38. Y. Liu, B. Cheng, K.-K. Wang, G.-P. Ling, J. Cai, C.-L. Song and G.-R. Han, *Solid State Commun.* , 2014, **178**, 16-22.
39. K. Leung, Y. Qi, K. R. Zavadil, Y. S. Jung, A. C. Dillon, A. S. Cavanagh, S. H. Lee and S. M. George, *J. Am. Chem. Soc.* , 2011, **133**, 14741-14754.

40. Y. Hu, A. Ruud, V. Miikkulainen, T. Norby, O. Nilsen and H. Fjellvåg, *RSC advances*, 2016, **6**, 60479-60486.
41. S.-Y. Kim, A. Ostadhossein, A. C. Van Duin, X. Xiao, H. Gao and Y. Qi, *PCCP* 2016, **18**, 3706-3715.
42. X.-Y. Yue, W.-W. Wang, Q.-C. Wang, J.-K. Meng, X.-X. Wang, Y. Song, Z.-W. Fu, X.-J. Wu and Y.-N. Zhou, *Energy Storage Materials*, 2019, **21**, 180-189.